Available online at www.sciencedirect.com
SCIENCE DIRECT
Applied Surface Science 252 (2006) 5499–5503
applied surface science
www.elsevier.com/locate/apsusc

Probing of local dissolution of Al-alloys in chloride solutions by AFM and SECM

A. Davoodi [a], J. Pan [a,*], C. Leygraf [a], S. Norgren [b]

[a] Div. Corrosion Science, School of Industrial Engineering and Management, Royal Institute of Technology, SE-100 44 Stockholm, Sweden
[b] Sapa Technology, SE-612 81 Finspång, Sweden

Available online 18 January 2006

Abstract

Local dissolution of Al alloys was probed in situ in chloride solutions by using atomic force microscopy (AFM) and scanning electrochemical microscopy (SECM). Preferential dissolution in the boundary region between some intermetallic particles (IMPs) and alloy matrix, and trench formation around large IMPs during free immersion and under electrochemical anodic polarization were observed, which indicate different dissolution behavior associated to different types of IMPs. Moreover, by using an integrated AFM/SECM system with a dual mode cantilever/microelectrode probe, simultaneous probing of electrochemical active sites and topographic changes over the same area was performed with sub-micron resolution. This allowed the ongoing localized corrosion processes related to the IMP to be revealed.

PACS: 82.45.Bb

Keywords: Localized corrosion; Al alloys; Intermetallic particles; EC-AFM and SECM

1. Introduction

In Al alloys, Si, Fe, Mn, Cr, Cu and Mg are introduced at various levels mainly to improve mechanical strength. Si and Fe are normally present as unavoidable impurities in commercially pure Al up to a total of 0.5 wt.%, but may also be introduced at higher levels. Various kinds of intermetallic precipitates (IMPs) may form in the alloys and their influence on corrosion processes has to be studied in detail, to understand the mechanism and, hence, to control the corrosion of the Al alloys. Detailed investigations are needed on initiation and formation of trenches around IMPs and pits at or near IMPs, and the influence of chemical composition and particle size of the IMPs. Such studies require local techniques with a high lateral resolution. Among many local techniques that have been applied during the past decade, atomic force microscopy (AFM) and scanning electrochemical microscopy (SECM) have shown great promises in the in situ study of localized corrosion of Al alloys. With a proper electrochemical setup, AFM measurements can be performed in aqueous solutions under electrochemical control (EC-AFM). Repeated AFM imaging of the surface can reveal trench formation and pitting initiation from the topographic change, whereas SECM mapping is capable to show local corrosion activity (e.g., anodic dissolution), appearing as electrochemically active sites.

AFM has been employed to study the role of Fe-rich IMPs such as Al_3Fe on pit initiation on Al alloys in aerated NaCl solution, whereby the topographic images showed cavity growth around IMPs [1]. Using a microelectrode and a redox mediator, SECM has been utilized to map local dissolution activity around MnS inclusions in stainless steels [2], and to spatially resolve heterogeneous cathodic activity at Al alloy (type AA2024) surfaces that was attributed to intermetallic particles [3]. However, the lateral resolution of the SECM used was not sufficiently high to obtain clear images of the local current. Recently, efforts have been made to integrate EC-AFM and SECM into one system, in order to obtain simultaneous topographic and electrochemical activity information on the same surface. The integrated EC-AFM/SECM has been used for characterization of Ti/TiO_2/noble metal anodes [4], mapping of enzyme activity [5] and biosensor surfaces [6].

* Corresponding author at: Drottning Kristinas Väg 51, SE-100 44 Stockholm, Sweden. Tel.: +46 8 790 6739; fax: +46 8 20 82 84.
E-mail address: jinshanp@kth.se (J. Pan).

0169-4332/$ – see front matter © 2005 Elsevier B.V. All rights reserved.
doi:10.1016/j.apsusc.2005.12.023

Table 1
Chemical composition (wt.%) of Al alloys investigated

Alloy	Si	Fe	Cu	Mn	Mg	Zn	Ti	Cr	Zr	Al
Pure Al	0.06	0.31	<0.01	<0.01	<0.01	0.01	0.01	–	–	Bal.
Al–Mn–Cu–Cr–Zr	0.04	0.16	0.57	1.46	0.26	0.01	0.02	0.11	0.12	Bal.
Al–Si	7.7	0.16	<0.01	<0.01	<0.01	<0.01	<0.01	<0.01	<0.01	Bal.

We have applied an integrated EC-AFM/SECM system for in situ investigation of localized corrosion of Al alloys in chloride solutions. Concurrent topography and electrochemical activity maps were obtained on the same surface area with micrometer resolution, showing ongoing localized dissolution related to IMPs in the alloys [7].

This paper presents results from AFM and SECM probing of local dissolution of Al alloys in chloride solution, including in situ AFM observation of preferential dissolution in the boundary between some IMPs and the matrix, and trench formation around large IMPs during free immersion and under electrochemical anodic polarization. One example is given of concurrent topographic and electrochemical activity on the same surface.

2. Experimental details

Commercial wrought Al alloys where used, pure Al, an Al–Si alloy and an Al–Mn–Cu–Cr–Zr core alloy (low in Si) onto which an Al–Si braze alloy was clad. The latter material combination, typically used in brazed heat exchanger applications for joining fin and tube systems, was exposed to a certain heat-treatment allowing the Al–Si alloy to melt. The compositions are given in Table 1. The alloy microstructure typically contains micrometer sized IMPs and also nanometer sized particles (dispersoids) distributed in the matrix, the latter type of fine particles are especially present in the Al–Mn–Cu–Cr–Zr alloy. In pure Al, the intermetallic components are Al_3Fe or AlFeSi-type phases. In the Al–Mn–Cu–Cr–Zr alloy, the particles are frequently of Al(Fe,Mn,Cr) type with minor Cu, and α-$Al_{12}(Mn,Fe)_3Si_{(1-2)}$ phase with Cu and Cr, which may be formed after the brazing heat treatment. These particles may be present both as IMPs and as submicron-sized dispersoids, and a few larger eutectic Al_3Fe IMPs may also be present. In the Al–Si alloy one finds predominantly AlFeSi phases along with eutectic Si particles.

The cut small samples were mounted in a low viscosity epoxy leaving 0.01–0.02 cm^2 exposed surface area. The sample surface was ground with SiC paper up to 4000 grit, and then polished with 1 and 0.25 μm diamond paste, using 99.5% ethanol. The sample was fixed in an electrochemical cell made of Teflon, with a large Pt foil counter electrode and a saturated Ag/AgCl reference electrode, Fig. 1a. The solution was added to the cell, so that the sample surface was covered by a solution layer about 2–3 mm thick. The solutions were made up using reagent NaCl, KI and distilled water. NaCl-containing solutions represent typical corrosive environments for Al alloys in many applications. KI was added to the solution as a redox mediator (I^-/I_3^- redox couple) when SECM measurements were performed [7]. All experiments were performed in aerated solutions.

The AFM instrument used was a Quesant Resolver, equipped with the iProbe packet supplied by Windsor Scientific Ltd., UK, for EC-AFM and integrated EC-AFM/SECM measurements. The iProbe packet includes a battery-driven, low noise and high current sensitivity (pico-A) bipotentiostat, for separate control of the potential of the sample and the microelectrode, and for measurement of the total electrochemical current through the sample and the local current through the microelectrode. For the EC-AFM measurements, a standard silicon nitride cantilever was mounted on a glass adaptor for liquid media before it was attached to the scanning head. The topographic imaging was then performed in a normal AFM mode while the sample was controlled at a constant potential, e.g., open-circuit potential or anodic potentials. For the integrated EC-AFM/SECM measurements, a specially

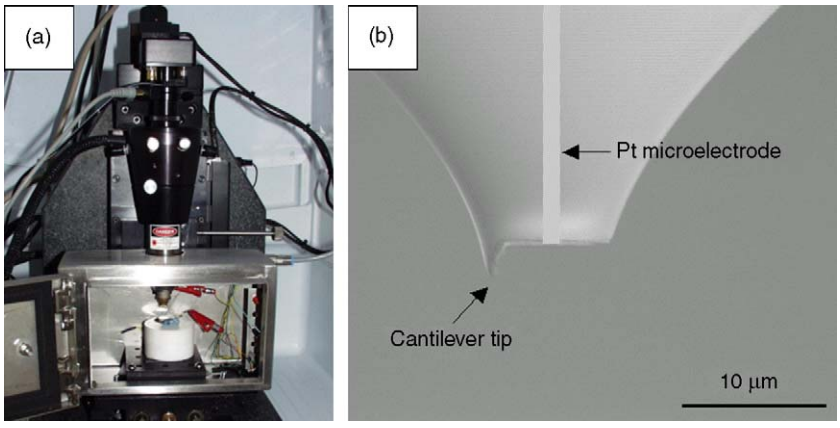

Fig. 1. (a) The AFM instrument and electrochemical cell. (b) The dual mode probe for integrated EC-AFM/SECM measurement.

fabricated dual mode probe was used, which functions both as the AFM cantilever and the SECM microelectrode. It was prepared by embedding a Pt wire in a long arm L shape cantilever, which was then insulated by epoxy. The arm was flattened and coated with gold for laser reflection, and the bending end was cut to form a cantilever tip and leave the Pt microelectrode exposed, Fig. 1b. During the measurement, the sample potential was controlled at anodic values at which local dissolution may occur on the Al alloy surface, while the potential of the Pt microelectrode was controlled at a predefined value for maximal collection of the local electrochemical current through the redox reactions. When scanning over the sample surface, the SECM line scan was performed at a preset distance (a few 100 nm to a few μm) directly after an AFM line scan, so that an AFM image and a SECM electrochemical current map were concurrently obtained on the same surface area. The lateral resolution of the SECM depends on the tip size, sample–electrode distance and the solution conductivity, and can reach micrometer level. More details of experimental procedure have been described elsewhere [7].

3. Results and discussion

Under free immersion, localized dissolution was hardly observed on surface of the Al alloys within several hours of the experiments, due to slow initiation and dissolution kinetics. Under anodic polarization of a few hundreds of mV, i.e., accelerated corrosion, localized dissolution was observed in a reasonable experimental time. Fig. 2 shows in situ AFM observation of localized corrosion of the Al–Si alloy under anodic polarization close to breakdown potential (ca. −550 mV versus Ag/AgCl) in 10 mM NaCl + 50 mM KI solution. Severe localized dissolution occurred in the boundary surrounding a round-shaped particle of about 1 μm size, Fig. 2a. In contrast, localized dissolution occurred between two irregular-shaped particles (1–2 μm size), while the boundary region to the matrix remains intact, Fig. 2b. The different dissolution behavior of the particle/matrix boundaries can be attributed to different types of IMPs.

Fig. 2c shows dissolution products deposited around a particle, due to enhanced local dissolution in the particle/matrix boundary region. The pit appearance is probably due to loss of the particle. Enhanced local dissolution of the matrix at the boundary of large IMPs and concomitant deposition of oxy-hydroxides around the particles were observed previously [8,9]. Fig. 2d shows a large ring in the area where severe local dissolution occurred between the particles. In highly corrosive but neutral media, such corrosion phenomena are accelerated and such rings may turn into distinct mm-sized cylindrical shaped tubes. During enhanced local dissolution, mass diffusion limits the reaction rate and leads to ionic saturation in vicinity of the active sites. This explains the observed deposition of corrosion products above and around IMPs. As expected, higher anodic polarization resulted in more corrosion products. Note that the details of deposition of corrosion products could only be observed by in situ measurements with a high lateral resolution, such as the EC-AFM facility of this study.

Continuous AFM probing of a section across the interface between the Al–Mn–Cu–Cr–Zr core and the brazed metal (former Al–Si cladding layer, formed after the brazing) for several hours revealed a sequence of trench formation, as exemplified in Fig. 3. The trench preferentially forms around some large IMPs (lighter color area) in the Al–Mn–Cu–Cr–Zr

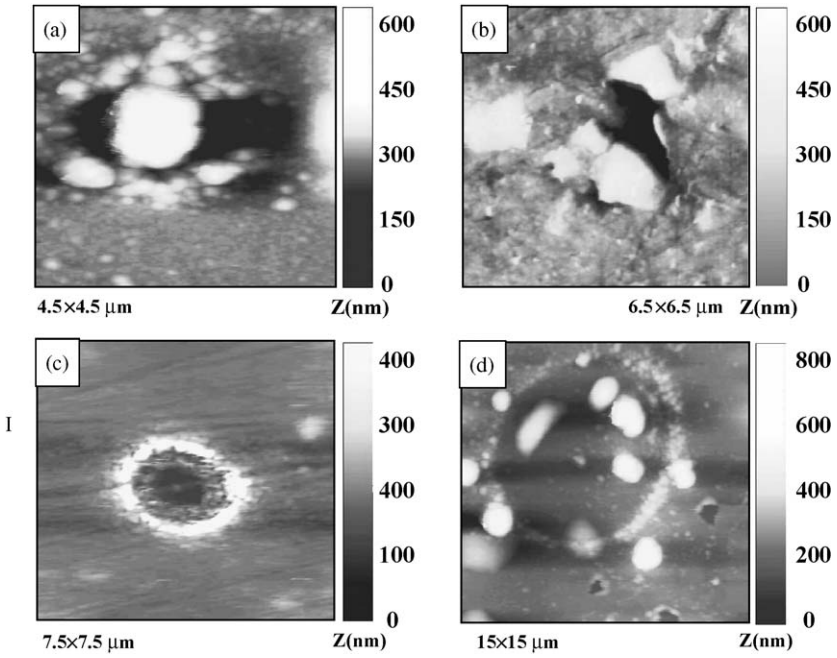

Fig. 2. EC-AFM topography of an Al–Si alloy under anodic polarisation close to breakdown potential in 10 mM NaCl + 50 mM KI solution; (a)–(d) different surface areas.

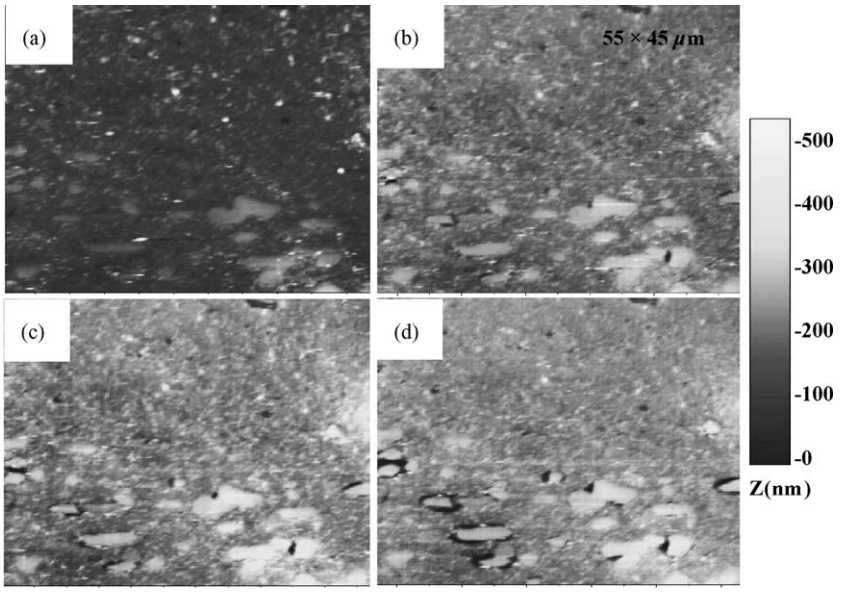

Fig. 3. In situ AFM topography of an Al–Mn–Cu–Cr–Zr alloy with an Al–Si braze cladding layer (after heat treatment at 600 °C) during free immersion in 10 mM NaCl + 50 mM KI solution for 6 h. Sequence from (a) to (d) show trench formation.

core, due to local dissolution of the matrix at the boundary of the IMPs. Often these attacks start at the narrow end of the elongated IMPs. The particle-free braze metal (upper part in Fig. 3a–d) of the former Al–Si alloy shows no sign of attack. The galvanic effect between the IMPs and the matrix leads to an enhanced local dissolution of the matrix at the boundary of large IMPs. Similar trench formation was observed adjacent to cathodic IMPs on polished AA 2024-T3, by in situ investigation using confocal laser scanning microscopy [9,10]. It was claimed that the oxide at the IMP/matrix interface would become less stable due to localized alkaline environment, as a results of the cathodic reaction at the particle surface increasing the OH^- activity [1,11].

By using the integrated AFM and SECM system with the dual mode probe, simultaneous probing of electrochemical active sites and topographic changes over the same area was carried out during the ongoing corrosion process of the Al alloys. The high-resolution images, typically of a few to tens of micrometers in dimension, reveal on-going localized dissolution associated with the IMPs in the alloys. It was observed that only a small fraction of the total number of the IMPs is involved in active dissolution at a given time. As an example, Fig. 4 presents concurrent AFM topography and SECM electrochemical current images (60 × 60 μm) obtained for the pure aluminium alloy at 50 mV anodic polarization in 10 mM NaCl + 5 mM KI solution. The line profiles under the 2D images show the variations in height and electrochemical activity. Although the resolution of the topography was not optimized due to the use of the dual mode probe, the images reveal high local current area (light color) on the surface in the electrochemical current map (Fig. 4b) even when there was no considerable height variation in the topography (Fig. 4a).

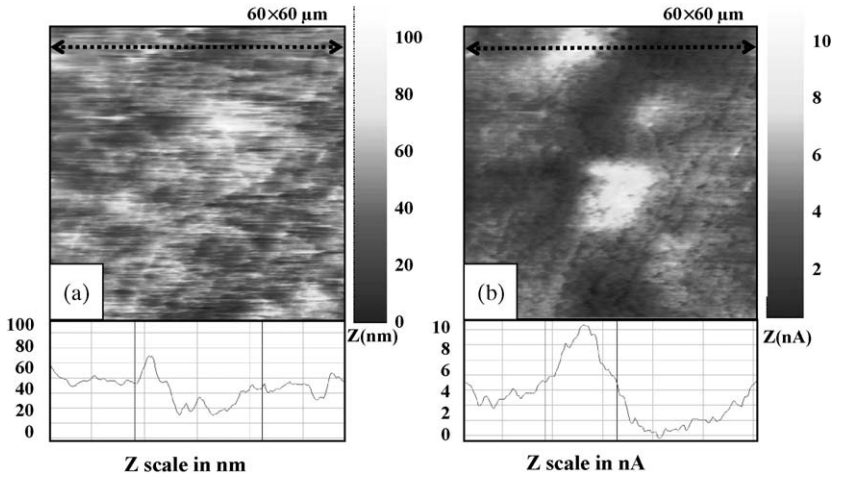

Fig. 4. Concurrent EC-AFM/SECM images obtained for pure aluminium in 10 mM NaCl + 5 mM KI at 50 mV anodic polarization. (a) AFM topography and line profile. (b) SECM electrochemical current map and line profile.

In this case, the maximum current was about 10 nA on two local areas (lighter) of less than 10 μm in dimension, as revealed by SECM mapping. These active sites (at least two are seen in the scanned area) indicate the weaker points of the passive oxide film on the Al alloy and are likely precursors of pitting sites in later stages.

4. Conclusions

Atomic force microscopy (AFM) and scanning electrochemical microscopy (SECM) have shown great promises for in situ probing of local dissolution, e.g., pitting and trench formation of Al alloys. A sequence of trench formation around large cathodic intermetallic particles (IMPs) was observed in situ by AFM in chloride solutions. Different local dissolution behavior in particle/matrix boundary regions was observed under anodic polarization (EC-AFM), which can be attributed to different types of IMPs. Moreover, by using an integrated AFM and SECM system with a dual mode cantilever/microelectrode probe, simultaneous probing of electrochemically active sites and topographic changes over the same area was accomplished during the ongoing corrosion process. The results reveal precursors for pitting of the Al alloys, and indicate that only a small fraction of IMPs is involved in the corrosion process at any given time.

Acknowledgements

Sapa Heat Transfer AB, Finspång, Sweden, and the Brinell Centre at the Royal Institute of Technology, Stockholm, Sweden, are acknowledged for the financial support. Dr. Yingyang Zhu of Windsor Scientific Ltd. is greatly acknowledged for assistance with the instrument and for valuable discussion.

References

[1] J.O. Park, C.H. Paik, Y.H. Huang, et al., Influence of Fe-rich intermetallic inclusions on pit initiation on aluminum alloys in aerated NaCl, J. Electrochem. Soc. 146 (1999) 517.
[2] C.H. Paik, H.S. White, R.C. Alkire, Scanning electrochemical microscopy detection of dissolved sulfur species from inclusions in stainless steel, J. Electrochem. Soc. 147 (2000) 4120.
[3] J.C. Seegmiller, D.A. Buttry, A SECM study of heterogeneous redox activity at AA2024 surfaces, J. Electrochem. Soc. 150 (2003) B413.
[4] J.P.G. de Mussy, J.V. Macpherson, J.L. Delplanck, Characterization and behaviour of Ti/TiO_2/noble metal anodes, Electrochim. Acta 48 (2003) 1131.
[5] H.C. Kranz, A. Kueng, A. Lugstein, et al., Mapping of enzyme activity by detection of enzymatic products during AFM imaging with integrated SECM–AFM probes, Ultramicroscopy 100 (2004) 127.
[6] Y. Hirata, S. Yabuki, F. Mizutani, Application of integrated SECM ultra-micro-electrode and AFM force probe to biosensor surfaces, Bioelectrochemistry 63 (2004) 217.
[7] A. Davoodi, J. Pan, C. Leygraf, et al., In situ investigation of localized corrosion of aluminum alloys in chloride solution using integrated EC-AFM/SECM techniques, Electrochem. Solid State Lett. 8 (2005) B21.
[8] T.L. Kuntson, F. Guillaume, W.J. Lee, et al., Reactivity of surfaces and imaging with functional NSOM, Electrochim. Acta 48 (2003) 3229.
[9] G.O. Ilevbare, O. Schneider, R.G. Kelly, et al., In situ confocal laser scanning microscopy of AA 2024-T3 corrosion metrology I. Localized corrosion of particles, J. Electrochem. Soc. 151 (2004) B453.
[10] O. Schneider, G.O. Ilevbare, J.R. Scully, et al., In situ confocal laser scanning microscopy of AA 2024-T3 corrosion metrology II. Trench formation around particles, J. Electrochem. Soc. 151 (2004) B465.
[11] D.B. Blücher, Carbon dioxide: the unknown factor in the atmospheric corrosion of light metals – a laboratory study, Doctoral Thesis, Chalmers University of Technology, Sweden, 2005.